Molecular BioSystems

Dynamic Article Links

Cite this: *Mol. BioSyst.*, 2011, **7**, 1990–1998

www.rsc.org/molecularbiosystems

PAPER

Plasma proteomic analysis of the critical limb ischemia markers in diabetic patients with hemodialysis

Peir-Haur Hung,†[ab] Yi-Wen Chen,†[c] Kuang-Chi Cheng,†[d] Hsiu-Chuan Chou,[e] Ping-Chiang Lyu,[c] Ying-Chieh Lu,[c] Ying-Ray Lee,*[f] Cheng-Tao Wu*[gh] and Hong-Lin Chan*[c]

Received 9th February 2011, Accepted 15th March 2011
DOI: 10.1039/c1mb05055a

Critical limb ischemia (CLI) is a severe obstruction of the arteries resulting from seriously decreased blood flow to the extremities, progressing to the point of pain and even skin ulcers or sores. CLI is associated with a high percentage of limb loss and mortality; however, no reliable biochemical indices are available to monitor the stages of CLI. We developed a strategy involving comparative proteomic analysis to detect CLI associated plasma biomarkers. 2D-DIGE and subsequent MALDI-TOF MS analyses provided 50 differentially expressed plasma proteins (including alkaline phosphatase and haptoglobin), between hemodialytic diabetic patients with and without CLI. Interestingly, more than half of the differentially expressed plasma proteins are associated with inflammatory responses. Our results show that CLI is strongly correlated to inflammation, indicating a strong potential for proteomics analysis in the diagnosis of CLI. To the best of our knowledge, this is the first report presenting a proteomics approach to monitor differentially expressed plasma proteins associated with CLI.

Introduction

Critical Limb Ischemia (CLI) is a severe obstruction of the arteries, resulting from seriously decreased blood flow to the extremities, progressing to the point of severe pain and even skin ulcers or sores, with a high incidence of limb loss and mortality. According to Norgren *et al.*'s study, 25% of patients have resolved CLI, 20% have ongoing CLI, 30% survive with limb amputation, and 25% die within one year following initial presentation with CLI.[1] In these, diabetes is a major contributor to CLI and the diabetic patients have 5 to 10 times more chance than non-diabetic patients to suffer from CLI due to diabetic neuropathy and altered immunoregulation by uncontrolled glycosylation.[2] Concomitantly, patients with end-stage renal disease (ESRD) who begin dialysis with foot lesions, such as CLI, face an increased risk of dying, independent of diabetes, and complications resulting from CLI rank among the main causes of death in patients with ESRD.[3] The goal of CLI therapy is to reduce cardiovascular risk factors, heal ulcers, relieve ischemic pain, prevent amputation, and increase the rate of survival. These aims can be achieved through revascularization, amputation, or other medical therapies.[4] Currently, several tests are applied to confirm the diagnosis of CLI, such as the ankle–brachial index and transcutaneous oxygen pressure. Incompressible arteries in the lower limbs and an ankle–brachial index >1.3 are independent predictors of limb amputation.[5] An ABI of <0.9 can predict mortality in advanced chronic kidney disease and patients receiving hemodialysis.[6,7] In addition, a reduction in transcutaneous oxygen pressure is an indication of impaired blood flow and a predictor of amputation.[8]

Two-dimensional gel electrophoresis (2-DE) and MALDI-TOF MS have been widely used to profile plasma proteins, and a number of the nonionic and zwitterionic detergents such

[a] *Division of Nephrology, Department of Internal Medicine, Chia-yi Christian Hospital, Chia-yi, Taiwan*
[b] *Department of Nursing, Chia-yi School, Chang Gung Institute of Technology, Chia-yi, Taiwan*
[c] *Institute of Bioinformatics and Structural Biology and Department of Medical Science, National Tsing Hua University, No. 101, Kuang-Fu Rd. Sec. 2, Hsin-chu, 30013, Taiwan. E-mail: hlchan@life.nthu.edu.tw; Fax: +886-3-5715934; Tel: +886-3-5742476*
[d] *Biological Function and Protein Engineering Laboratory, Strategic Business and Innovation Technology Development Division, Biomedical Technology and Device Research Laboratory, Industrial Technology Research Institute, Hsinchu, Taiwan*
[e] *Department of Applied Science, National Hsinchu University of Education, Hsinchu, Taiwan*
[f] *Department of Medical Research, Chiayi Christian Hospital, No. 539, Jhongsiao Rd., Chiayi, Taiwan. E-mail: yingray.lee@gmail.com; Fax: +886-5-2765041 ext. 1094; Tel: +886-5-2765041 ext. 5560*
[g] *Biomedical Informatics Laboratory, Strategic Business and Innovation Technology Development Division, Biomedical Technology and Device Research Laboratory, Industrial Technology Research Institute, Hsinchu, Taiwan. E-mail: ct.carton.wu@itri.org.tw; Tel: +886-3-5820100*
[h] *Institute of Biomedical Informatics, National Yang-Ming University, Taipei, Taiwan*
† These authors contributed equally to this work.

as thiourea and CHAPS have been introduced to increase the solubility of plasma proteins. Gel-based detection and quantification of proteins has been significantly improved since the introduction of 2D-DIGE, enabling the co-detection of numerous samples in the same 2-DE. This minimizes gel-to-gel variation, and facilitates the comparison of protein characteristics among different gels, according to an internal fluorescent standard. This innovative technology relies on the pre-labeling of protein samples prior to electrophoresis with fluorescent dyes Cy2, Cy3, and Cy5, each of which exhibits a distinct fluorescent wavelength allowing the inclusion of multiple samples, for use as internal standards. In this manner, samples can be simultaneously separated within a single gel. An internal standard, which is a pool of an equal number of protein samples, enhances the accuracy of data associated with normalization and increases statistical confidence in quantitation across gels.[9–14]

Several strategies such as the measurement of the ankle–brachial index and transcutaneous oxygen pressure have been developed to monitor the stages of CLI. However, in several instances, these methods have failed to detect cases of CLI, which have been later proven by clinical diagnosis.[15] Clearly, developing new techniques to detect CLI is essential for both early diagnosis and eventual prognosis. Proteomics is a powerful tool for the analysis of complex mixtures of proteins and the identification of biomarkers. To examine differentially expressed levels of plasma proteins associated with CLI, we developed a proteomics-based approach involving immuno-depletion of high abundance proteins, 2D-DIGE analysis, and subsequent MALDI-TOF MS analysis to obtain a panel of plasma proteins, differentially expressed between hemodialytic diabetic patients with and without CLI.

Results

Plasma sample preparation

Demographic information is shown in Table 1. CLI was monitored following clinical diagnosis. No significant difference in age (58.80 ± 7.05 years *versus* 58.00 ± 1.87 years) or anemia (serum hemoglobulin levels: 10.70 ± 0.96 g dL^{-1} *versus* 11.74 ± 2.01) was noted between patients with and without CLI. The known durations of diabetes (10.42 ± 4.80 years *versus* 10.25 ± 1.61 years) and dialysis (7.87 ± 3.70 years *versus* 4.82 ± 3.61 years) were similar in hemodialytic diabetic subjects with CLI. There was no significant difference in serum creatinine levels, serum CRP levels, body weight, or body mass index among patients with CLI.

Table 1 Clinical parameters for diabetic hemodialytic patients with/without critical limb ischemia participating in this investigation (values are mean ± SD). The values in this table are calculated with the Student's *t* test. The abbreviations used in this table: Hb, hemoglobulin; Cr, chromium; *Kt*/*V*, (dialyzer clearance of urea × dialysis time)/volume of distribution of urea; CRP, C-reactive protein; BW, body weight; BMI, body mass index; DM duration, diabetes mellitus duration

	CLI	Non-CLI
Age/years	58.80 ± 7.05	58.00 ± 1.87
Hb/g dL^{-1}	10.70 ± 0.96	11.74 ± 2.01
Cr/mg dL^{-1}	9.18 ± 1.81	11.64 ± 1.69
Kt/*V*	1.66 ± 0.11	1.59 ± 0.13
CRP/mg dL^{-1}	1.84 ± 2.92	0.16 ± 0.22
BW/kg	57.82 ± 8.72	64.01 ± 9.08
BMI/kg m^{-2}	21.64 ± 2.46	23.81 ± 2.93
DM duration/years	10.42 ± 4.80	10.25 ± 1.61
Dialysis duration/years	7.87 ± 3.70	4.82 ± 3.61

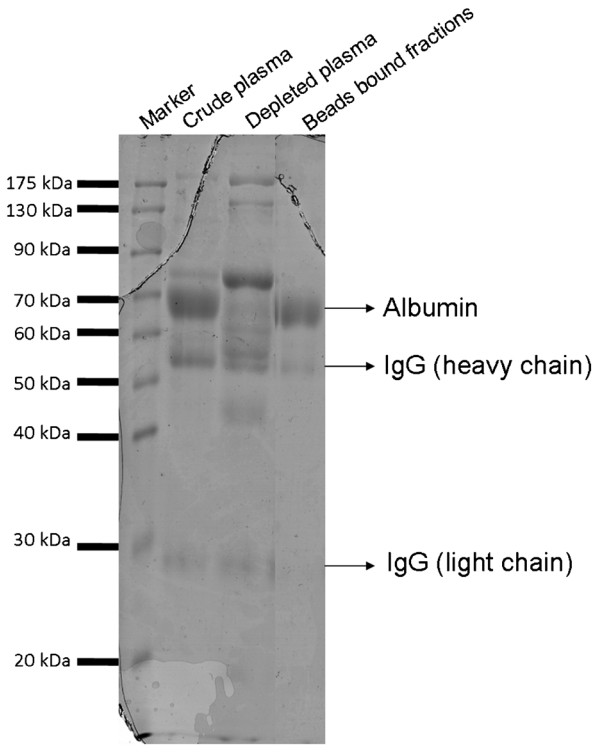

Fig. 1 Efficiency evaluation of the removal of albumin and immunoglobulin G from plasma samples. 20 μg of the crude plasma, albumin and immunoglobulin-depleted plasma and beads bound protein fractions were loaded and resolved by SDS-PAGE followed by staining with colloidal coomassie blue G-250.

Because albumin and immunoglobulin G account for approximately 70–80% of the proteins in human plasma, these highly abundant proteins represent an obstacle to 2-DE analysis. Consequently, removing (high-abundance) albumin and immunoglobulin G from plasma samples can increase the viability of low- and middle-abundance proteins, enabling more accurate analysis. In this study, the high abundance proteins were removed using an albumin and IgG removal kit, prior to 2D-DIGE analysis, and the effect of depletion was evaluated using 1D-SDS-PAGE (Fig. 1).

2D-DIGE and mass spectrometry analyses of the immunodepleted plasma proteome

To study alterations in plasma proteins in patients with critical limb ischemia, comparative proteomic analysis was performed between patients with and without CLI. 2-DE images of the samples of two groups were minimally labeled using Cy3 and Cy5 dyes and distributed on each gel. A pool of both samples was also prepared for labeling with Cy2 as an internal standard for all gels, to facilitate image matching across each

A

	Cy2 (50μg)	Cy3 (50μg)	Cy5 (50μg)
Gel1	Pool	Non-CLI	CLI
Gel2	Pool	CLI	Non-CLI
Gel3	Pool	Non-CLI	CLI

B

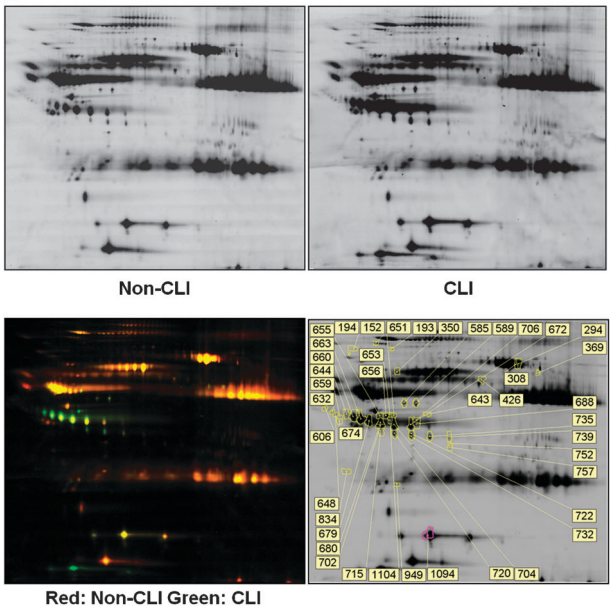

Fig. 2 2D-DIGE analysis of critical limb ischemia-induced differentially expressed proteins. (A) Arrangement of plasma samples for a 2D-DIGE experiment in triplicate. (B) Plasma samples (50 μg each) were labeled with Cy-dyes and separated using 24 cm, pH 3–10 non-linear IPG strips. 2D-DIGE images of the plasma samples from patients with and without critical limb ischemia at appropriate excitation and emission wavelengths are shown (top) as well as overlain pseudo-colored images processed with ImageQuant Tool (GE Healthcare) (left bottom). Differentially expressed identified protein features are annotated with spot numbers (right bottom).

of the gels. The arrangement of plasma samples for a triplicate 2D-DIGE experiment is shown in Fig. 2A. Thus, samples were resolved in different gels in triplicate, enabling quantitative analysis using the internal standard on multiple 2-DE. After resolving the protein samples with the 2D-DIGE technique, DeCyder image analysis software indicated that 107 protein features showed greater than a 1.5-fold change in abundance, with a Student *t*-test *p*-value of less than 0.05. 2D-DIGE analysis and MALDI-TOF MS identification revealed a differential abundance of 50 proteins between CLI and non-CLI samples (Fig. 2B, Fig. 3 and Table 2). Most of the identified proteins were secreted proteins (70%), cytoplasmic proteins (12%) and plasma membrane proteins (8%). These proteins are associated with inflammatory response (54%), transportation (16%) and cytoskeleton (8%) (Fig. 4). Fig. 5 illustrates representative changes in the abundance of critical limb ischemia-dependent proteins following quantitative evaluation of alterations in spot intensity using the 2D-DIGE system. The location of selected proteins such as protein FAM55D, fibrinogen, alkaline phosphatase, leucine-rich α-2-glycoprotein, haptoglobin, and 14-3-3 protein zeta/delta

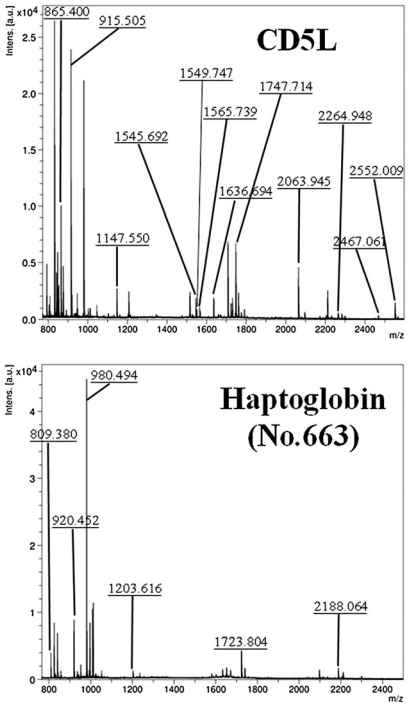

Fig. 3 Peptide fingerprinting of identified proteins CD5L and haptoglobin.

is shown on 2-DE maps, with standardized changes in abundance using three-dimensional spot images and graphical images (Fig. 5).

Validation by immunoblotting and ELISA

The abundance of haptoglobin was determined by immunoblotting to verify the abundance of proteins obtained from 2D-DIGE and MALDI-TOF MS. As shown in Fig. 6A, the 46 kDa of haptoglobin was increased in the plasma of patients with critical limb ischemia. We also performed an ELISA assay to verify proteomic results, indicating significant increases in the level of haptoglobin, 14-3-3 protein zeta, and leucine-rich α-2-glycoprotein in patients with critical limb ischemia, compared to those without (Fig. 6B). The results of immunoblotting and ELISA were consistent with the data from the 2D-DIGE and MALDI-TOF MS, further suggesting that the identified proteins could be employed as markers for the early diagnosis of critical limb ischemia.

Discussion

Proteomic analysis of human diseases is usually a comparative process defining the differential abundance of proteins associated with diseases in various stages. Because CLI is a vascular disease and a differential abundance of plasma proteins can be anticipated, we investigated the proteomics of the CLI in diabetic patients with hemodialysis. 2D-DIGE/MALDI-TOF analysis revealed 50 changes in the abundance corresponding to 23 unique plasma proteins (Table 2). Most of the altered proteins belonged to two major functional groups, inflammatory response and transport, while other affected categories included cytoskeleton, signal transduction, gene regulation,

Table 2 Alphabetical list of critical limb ischemia-induced differentially expressed plasma proteins identified by MALDI-TOF peptide mass fingerprinting following 2D-DIGE analysis

No.	Swiss-prot no.	Protein name	p*I*	MW	No. match. peptides	Cov.	Score	*t*-Test	CLI/non-CLI	Subcellular location	Functional ontology
834	P63104	14-3-3 protein zeta/delta	4.73	27 899	6/13	20%	74/56	0.0038	2.7	Cytoplasm	Signal transduction
369	Q86TM9	Acetylcholinesterase	5.87	68 209	6/16	12%	58/56	8.50×10^{-5}	2.69	Plasma membrane	Neural transmission
653	P60709	Actin, cytoplasmic 1	5.29	42 052	8/39	26%	81/56	0.012	4.32	Cytoplasm	Cytoskeleton
656	P60709	Actin, cytoplasmic 1	5.29	42 052	10/29	33%	102/56	0.00026	4.49	Cytoplasm	Cytoskeleton
1094	P05187	Alkaline phosphatase, placental type/PLAP-1	5.87	58 259	6/15	13%	59/56	0.00014	2.03	Plasma membrane	Metabolism
193	P12814	α-Actinin-1	5.25	1×10^5	9/13	9%	63/56	0.0059	2.97	Cytoplasm	Cytoskeleton
653	P06727	Apolipoprotein A-IV/APOA 4	5.28	45 371	8/39	20%	76/56	0.012	4.32	Secreted	Transport
672	P06727	Apolipoprotein A-IV/APOA 4	5.28	45 371	7/22	21%	63/56	0.017	2.37	Secreted	Transport
688	P06727	Apolipoprotein A-IV/APOA 4	5.28	45 371	7/21	21%	65/56	0.0051	2.17	Secreted	Transport
1104	O43866	CD5 antigen-like/CD5L/SP-alpha	5.28	39 603	12/32	45%	127/56	0.026	2.24	Secreted	Apoptosis
653	Q9UN19	Dual adapter for phosphotyrosine and 3-phosphotyrosine and 3-phosphoinositide/DAPP1/B lymphocyte adapter protein Bam32	7.66	32 458	5/12	23%	57/56	0.012	4.32	Plasma membrane	Inflammatory response
152	Q9UJM3	ERBB receptor feedback inhibitor 1/Mig-6	8.38	51 155	6/15	21%	58/56	0.0002	1.58	Cytoplasm	Signal transduction
732	Q9Y2P4	Fatty acid transport protein 6/FATP6/SLC27A6	8.75	70 865	7/22	15%	57/56	2.70×10^{-6}	4.15	Plasma membrane	Transport
585	P02679	Fibrinogen gamma chain	5.37	52 106	7/16	19%	78/56	8.90×10^{-5}	2.23	Secreted	Inflammatory response
589	P02679	Fibrinogen gamma chain	5.37	52 106	9/19	29%	110/56	7.70×10^{-5}	2.47	Secreted	Inflammatory response
752	O75636	Ficolin-3	6.2	33 395	6/20	14%	63/56	0.028	2.15	Secreted	Inflammatory response
660	Q9HD64	G antigen family D member 2/XAGE-1	9.76	18 196	4/23	36%	58/56	4.50×10^{-5}	5.75	NA	Unknown
426	Q9UHL9	General transcription factor II-I repeat domain-containing protein 1/GTF2IRD1	6.45	1×10^5	7/20	10%	59/56	1.30×10^{-3}	1.51	Nucleus	Gene regulation
643	P00738	Haptoglobin	6.13	45 861	5/12	10%	61/56	0.014	5.03	Secreted	Inflammatory response
644	P00738	Haptoglobin	6.13	45 861	9/21	19%	74/56	0.00023	6.03	Secreted	Inflammatory response
655	P00738	Haptoglobin	6.13	45 861	10/42	21%	61/56	0.00051	3.34	Secreted	Inflammatory response
660	P00738	Haptoglobin	6.13	45 861	10/32	21%	89/56	4.50×10^{-5}	5.75	Secreted	Inflammatory response
663	P00738	Haptoglobin	6.13	45 861	6/24	16%	58/56	1.10×10^{-5}	5.15	Secreted	Inflammatory response
679	P00738	Haptoglobin	6.13	45 861	6/20	14%	60/56	3.00×10^{-6}	4.39	Secreted	Inflammatory response
688	P00738	Haptoglobin	6.13	45 861	10/35	22%	79/56	0.0051	2.17	Secreted	Inflammatory response
702	P00738	Haptoglobin	6.13	45 861	7/26	18%	69/56	3.90×10^{-5}	3.44	Secreted	Inflammatory response
704	P00738	Haptoglobin	6.13	45 861	11/31	23%	92/56	6.80×10^{-6}	2.56	Secreted	Inflammatory response
706	P00738	Haptoglobin	6.13	45 861	7/17	14%	86/56	0.00019	1.95	Secreted	Inflammatory response
715	P00738	Haptoglobin	6.13	45 861	7/17	16%	66/56	5.70×10^{-5}	5.23	Secreted	Inflammatory response
720	P00738	Haptoglobin	6.13	45 861	7/25	20%	75/56	1.10×10^{-5}	5.07	Secreted	Inflammatory response
722	P00738	Haptoglobin	6.13	45 861	11/30	25%	88/56	1.60×10^{-5}	4.11	Secreted	Inflammatory response
732	P00738	Haptoglobin	6.13	45 861	11/35	25%	81/56	2.70×10^{-6}	4.15	Secreted	Inflammatory response
735	P00738	Haptoglobin	6.13	45 861	11/33	25%	84/56	1.10×10^{-6}	2.82	Secreted	Inflammatory response
739	P00738	Haptoglobin	6.13	45 861	11/35	25%	81/56	0.00033	1.86	Secreted	Inflammatory response
757	P00738	Haptoglobin	6.13	45 861	7/23	18%	59/56	5.30×10^{-5}	4.01	Secreted	Inflammatory response
1094	P00738	Haptoglobin	6.13	45 861	6/24	17%	71/56	0.00014	2.03	Secreted	Inflammatory response
949	P01834	Ig kappa chain C region	5.58	11 773	3/28	48%	62/56	0.001	2.5	Secreted	Immune response
606	P02750	Leucine-rich α-2-glycoprotein/LRG1	6.45	38 382	5/19	20%	63/56	0.023	1.54	Secreted	Inflammatory response

Table 2 (*continued*)

No.	Swiss-prot no.	Protein name	p*I*	MW	No. match. peptides	Cov.	Score	*t*-Test	CLI/non-CLI	Subcellular location	Functional ontology
632	P02750	Leucine-rich α-2-glycoprotein/ LRG1	6.45	38 382	8/25	34%	95/56	0.00084	1.58	Secreted	Inflammatory response
648	P02750	Leucine-rich α-2-glycoprotein/ LRG1	6.45	38 382	8/27	32%	88/56	0.00031	1.63	Secreted	Inflammatory response
659	P02750	Leucine-rich α-2-glycoprotein/ LRG1	6.45	38 382	6/20	23%	65/56	0.00026	1.96	Secreted	Inflammatory response
674	P02750	Leucine-rich α-2-glycoprotein/ LRG1	6.45	38 382	7/26	23%	74/56	0.031	1.85	Secreted	Inflammatory response
194	Q6UWF7	Protein FAM55D	9.03	62 850	6/9	14%	58/56	0.034	2.91	Secreted	Unknown
294	P02787	Serotransferrin	6.81	79 280	15/35	21%	91/56	0.00016	−1.59	Secreted	Transport
308	P02787	Serotransferrin	6.81	79 280	23/47	34%	196/56	0.0076	−1.5	Secreted	Transport
350	P02787	Serotransferrin	6.81	79 280	15/34	23%	125/56	0.0083	1.5	Secreted	Transport
704	Q13190	Syntaxin-5	9.21	39 762	5/7	19%	58/56	6.80×10^{-6}	2.56	ER	Transport
680	P68371	Tubulin β-2C chain	4.79	50 255	5/6	16%	61/56	9.10×10^{-6}	3.26	Cytoplasm	Cytoskeleton
655	O43172	U4/U6 small nuclear ribonucleo-protein Prp4	7.05	59 097	8/36	21%	58/56	0.00051	3.34	Nucleus	Gene regulation
651	Q6X4T0	Uncharacterized protein C12orf54	8.66	14 590	5/14	39%	57/56	0.0083	2.54	NA	Unknown

Fig. 4 Percentage of plasma proteins identified from albumin and immunoglobulin G depleted plasma by 2D-DIGE/MALDI-TOF MS for critical limb ischemia according to biological function (A) and subcellular location (B).

neural transmission, apoptosis, immune response, and metabolism (Fig. 4). Of these, 54% participate in various inflammatory pathways including B lymphocyte adapter protein Bam32 (regulating B-cell receptor signaling), fibrinogen gamma (platelet aggregation), ficolin-3 (innate immunity-dependent), haptoglobin (acute phase reactant), Ig kappa chain (humoral immunity) and leucine-rich α-2-glycoprotein (granulocyte differentiation). In previous studies, the up-regulation of plasma inflammatory molecules was associated with CLI and CLI-induced mortality.[16–18] By using immunomodulation therapy, CLI symptoms significantly improved and the incidence of CLI-induced limb amputation decreased considerably.[19] Thrombospondin-1 has been found to be highly expressed in ischemic tissue during CLI in humans and a deficiency of thrombospondin-1 can modulate macrophage activation preventing CLI-induced tissue necrosis.[20] Our proteomic analysis showed that more than half of the differentially expressed plasma proteins identified in this study are inflammation-related, and this result is strongly correlated with those of previous investigations. Fibrinogen, a precursor of fibrin, has been reported as an early diagnostic biomarker of ischemia,[21,22] and high mortality resulting from CLI has been shown to be associated with high levels of fibrinogen in a large scale study of patients with CLI.[23] A comparison between these studies on fibrinogen and our 2D-DIGE results shows that 2D-DIGE has potential to facilitate the identification of plasma disease markers with a reasonable degree of reproducibility. Haptoglobin binds free plasma hemoglobin, allowing degradative enzymes to decompose the hemoglobin. Haptoglobin has long been reported as a biomarker for

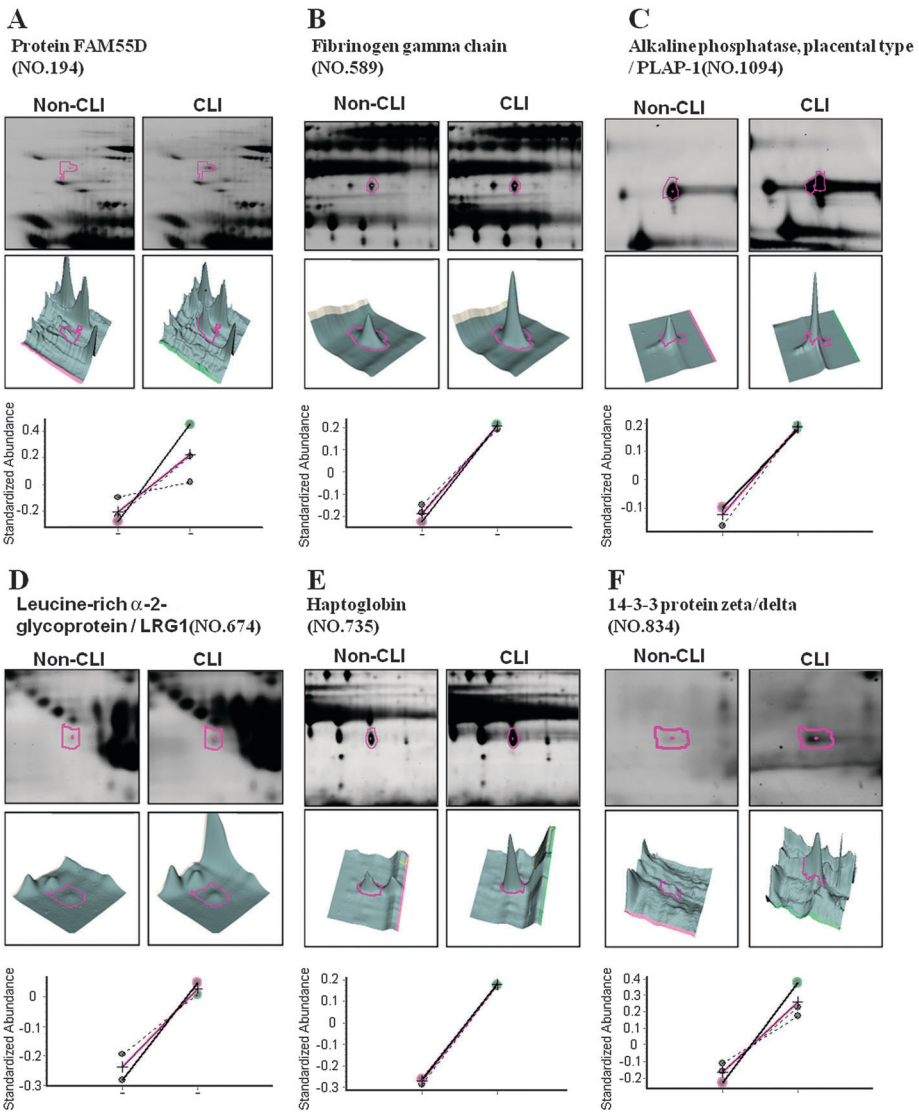

Fig. 5 Representative images of the identified spots ((A) protein FAM55D; (B) fibrinogen; (C) alkaline phosphatase; (D) leucine-rich α-2-glycoprotein; (E) haptoglobin; (F) 14-3-3 protein zeta/delta) displaying critical limb ischemia-dependent changes in the abundance of proteins. The levels of these proteins were visualized by 2-DE images (top panels), three-dimensional spot images (middle panels), and protein abundance maps (bottom panels).

chronic inflammation associated with atherothrombotic ischemic stroke,[24] forebrain ischemia,[25] arteriosclerosis[26] and angiogenesis[27] suggesting that haptoglobin might play a regulatory role in CLI.

Numerous identified CLI-related plasma proteins have been shown to play a role in other forms of ischemia; however, they have not been associated with CLI. These proteins include 14-3-3 protein,[28] acetylcholinesterase,[29] alkaline phosphatase,[30,31] apolipoprotein A-IV,[32] ficolin,[33] leucine-rich α-2-glycoprotein, and syntaxin.[34] Because CLI is caused by severe ischemia and inflammation, we suggest that these identified plasma proteins are potential candidates for use in the diagnosis of CLI. In contrast, other identified plasma proteins (CD5 antigen-like, dual adapter for phosphotyrosine and 3-phosphotyrosine and 3-phosphoinositide (DAPP1), erbB receptor feedback inhibitor 1 (Mig-6), fatty acid transport protein 6, G antigen family D member 2, general transcription factor II-I repeat domain-containing protein 1 and U4/U6 small nuclear ribonucleoprotein Prp4) have not been associated with CLI or other forms of ischemia, warranting further investigation to clarify their roles in CLI and evaluate their potential as CLI biomarkers.

Both protein–energy malnutrition and systemic inflammation are highly prevalent in patients with ESRD (end-stage renal disease), and further associated with a substantial increase in the risk of mortality.[35,36] Because malnutrition, inflammation, and atherosclerotic vascular disease often coexist, these risk factors have been proposed to be pathophysiologically linked.[37,38] A combination of these factors has previously been referred to as the malnutrition, inflammation, and atherosclerosis (MIA) syndrome.[39] In a present study, we showed that patients with CLI suffer from more severe

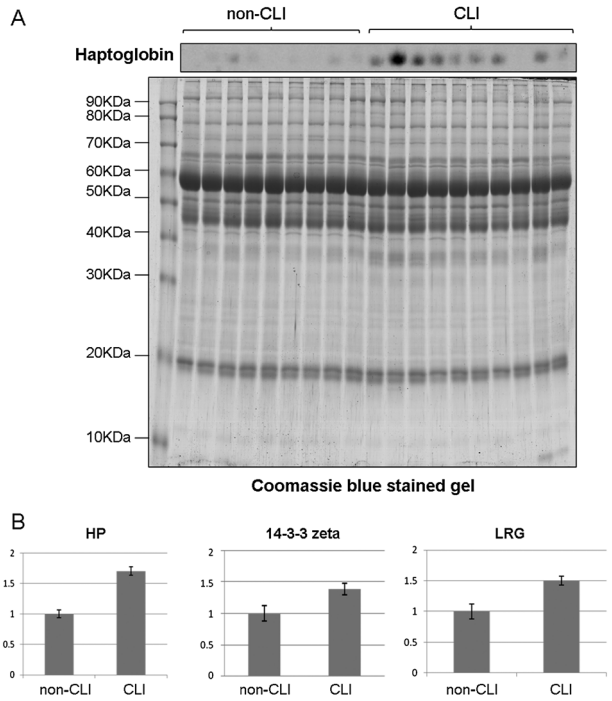

Fig. 6 Representative immunoblotting analysis of haptoglobin (A) and ELISA analysis of haptoglobin, 14-3-3 protein zeta and leucine-rich α-2-glycoprotein (B) for selected differentially expressed plasma proteins identified by proteomic analysis in patients with and without critical limb ischemia. (A) 20 μg of the albumin and immunoglobulin-depleted plasma were loaded and resolved by SDS-PAGE followed by either immunoblotting with haptoglobin or staining with colloidal coomassie blue G-250 as an internal loading control. (B) 50 μg of plasma samples were coated onto each well of a 96-well plate for ELISA analysis, and absorbance was measured at 450 nm using a Stat Fax 2100 microtiterplate reader.

MIA syndrome than non-CLI subjects. Clinically, this is inconsistent with our results involving proteomic analysis.

Our proteomic analysis of CLI is the first such report in this field. 2D-DIGE and MALDI-TOF MS have provided a powerful new approach to the proteomic analysis of human disease; however, this strategy has never been applied in the field of CLI. In this study, we developed a plasma proteomics strategy to identify potential markers for CLI.

The isolation of low-abundance proteins from plasma is often complicated due to high abundance proteins such as serum albumin and immunoglobulin. Serum albumin and immunoglobulin are the two most abundant proteins in plasma, comprising 60–90% of the plasma proteins. These proteins mask low-abundance proteins and limit the quantity of total plasma proteins that can be resolved by proteomic analysis. To remove these two high-abundance proteins, we used albumin and the IgG depletion kit from Sigma-Aldrich, containing prepacked spin columns, allowing the removal of most of the serum albumin and immunoglobulin. We also used trichloroacetic acid/acetone to precipitate, desalt, and enrich the plasma proteins to ensure that they are well resolved using 2D-DIGE. Our results demonstrate that this strategy prepared and separated the plasma proteins very effectively.

Conclusions

In conclusion, quantitative plasma proteomics analysis provides a valuable contribution to CLI research. Our results indicate that plasma inflammatory proteins (such as haptoglobin), ischemia related proteins (such as alkaline phosphatase) and a number of the other identified plasma proteins (such as DAPP1) are correlated with the CLI, and have the potential to serve as biomarkers for monitoring the course of the disease. The potential offered by these markers for the screening and treating of CLI warrants further investigation.

Materials and methods

Chemicals and reagents

Generic chemicals and albumin and IgG depletion kit were purchased from Sigma-Aldrich (St. Louis, USA), while reagents for 2D-DIGE were purchased from GE Healthcare (Uppsala, Sweden). All primary antibodies were purchased from Abcam (Cambridge, UK) and anti-mouse, anti-goat and anti-rabbit horseradish peroxidase conjugated secondary antibodies were purchased from GE Healthcare (Uppsala, Sweden). All the chemicals and biochemicals used in this study were of analytical grade.

Plasma sample collection and purification

From Jan 2009 to Dec 2009, ten diabetic patients with chronic hemodialysis in a single center (Chiayi Christian Hospital, Chiayi, Taiwan) were enrolled in the study. Those included in the study were divided into a CLI group ($n = 10$) and non-CLI group ($n = 9$). CLI was diagnosed if angiography showed one or more of stenosis, slow flow phenomenon, rarefication of one or more of the peripheral arteries and if patients had ulceration or gangrene. This study was approved by the Institutional Research Board and carried out according to the Helsinki Declaration Principles. Written informed consent was collected from all participating subjects. The clinical data of patients were measured in the clinical laboratory and are summarized in Table 1.

To improve the performance of proteomic analysis of the plasma samples, the albumin and immunoglobulin G in the collected plasma samples were depleted using an Albumin and IgG removal kit (Sigma, St. Louis, USA) in accordance with the manufacturer's instructions. The depleted plasma samples were precipitated by adding 1 volume of 100% TCA (at −20 °C) to 4 volumes of the sample and incubated for 10 min at 4 °C. The precipitated protein was then recovered by centrifugation at 13 000 rpm for 10 min, and the resulting pellet was washed twice with ice-cold acetone. Air-dried pellets were resuspended in 2-DE lysis containing 4% w/v CHAPS, 7 M urea, 2 M thiourea, 10 mM Tris-HCl, pH 8.3, 1 mM EDTA.

Sample preparation for 2D-DIGE and gel image analysis

The plasma protein pellets were dissolved in 2-DE lysis buffer and protein concentrations were determined using a Coomassie Protein Assay Reagent (BioRad). Before performing 2D-DIGE, protein samples were labeled with *N*-hydroxy

succinimidyl ester-derivatives of the cyanine dyes Cy2, Cy3 and Cy5 following the protocol described previously.[40,41] Briefly, 150 μg of the protein sample was minimally labeled with 375 pmol of either Cy3 or Cy5 for comparison on the same 2-DE. To facilitate image matching and cross-gel statistical comparison, a pool of all samples was also prepared and labeled with Cy2 at a molar ratio of 2.5 pmol Cy2 per microgram of protein as an internal standard for all gels. Thus, the triplicate samples and the internal standard could be run and quantified on multiple 2-DE. The labeling reactions were performed in the dark on ice for 30 min and then quenched with a 20-fold molar ratio excess of free L-lysine to dye for 10 min. The differentially Cy3- and Cy5-labeled samples were then mixed with the Cy2-labeled internal standard and reduced with dithiothreitol for 10 min. IPG buffer, pH 3–10 nonlinear (2% (v/v), GE Healthcare), was added and the final volume was adjusted to 450 μl with 2D-lysis buffer for rehydration. The rehydration process was performed with immobilized non-linear pH gradient (IPG) strips (pH 3–10, 24 cm) which were later rehydrated by CyDye-labeled samples in the dark at room temperature overnight (at least 12 hours). Isoelectric focusing was then performed using a Multiphor II apparatus (GE Healthcare) for a total of 62.5 kV h at 20 °C. Strips were equilibrated in 6 M urea, 30% (v/v) glycerol, 1% SDS (w/v), 100 mM Tris-HCl (pH 8.8), 65 mM dithiothreitol for 15 min and then in the same buffer containing 240 mM iodoacetamide for another 15 min. The equilibrated IPG strips were transferred onto 26 × 20 cm 12.5% polyacrylamide gels cast between low fluorescent glass plates. The strips were overlaid with 0.5% (w/v) low melting point agarose in a running buffer containing bromophenol blue. The gels were run in an Ettan Twelve gel tank (GE Healthcare) at 4 Watts per gel at 10 °C until the dye front had completely run off the bottom of the gels. Afterward, the fluorescence 2-DE was scanned directly between the low fluorescent glass plates using an Ettan DIGE Imager (GE Healthcare). This imager is a charge-coupled device-based instrument that enables scanning at different wavelengths for Cy2-, Cy3-, and Cy5-labeled samples. Gel analysis was performed using DeCyder 2-D Differential Analysis Software v7.0 (GE Healthcare) to co-detect, normalize and quantify the protein features in the images. Features detected from non-protein sources (*e.g.* dust particles and dirty backgrounds) were filtered out. Spots displaying a 1.5 average-fold increase or decrease in abundance with a p-value of <0.05 were selected for protein identification.

Protein staining

Colloidal coomassie blue G-250 staining was used to visualize CyDye-labeled protein features in 2-DE. Bonded gels were fixed in 30% v/v ethanol, 2% v/v phosphoric acid overnight, washed three times (30 min each) with ddH_2O and then incubated in 34% v/v methanol, 17% w/v ammonium sulfate, 3% v/v phosphoric acid for 1 h, prior to adding 0.5 g l^{-1} coomassie blue G-250. The gels were then left to stain for 5–7 days. No destaining step was required. The stained gels were then imaged on an ImageScanner III densitometer (GE Healthcare), which processed the gel images as .tif files.

In-gel digestion

Excised post-stained gel pieces were washed three times in 50% acetonitrile, dried in a SpeedVac for 20 min, reduced with 10 mM dithiothreitol in 5 mM ammonium bicarbonate pH 8.0 (Ammonium bicarbonate) for 45 min at 50 °C and then alkylated with 50 mM iodoacetamide in 5 mM ammonium bicarbonate for 1 h at room temperature in the dark. The gel pieces were then washed three times in 50% acetonitrile and vacuum-dried before reswelling with 50 ng of modified trypsin (Promega) in 5 mM ammonium bicarbonate. The pieces were then overlaid with 10 μl of 5 mM ammonium bicarbonate and trypsinized for 16 h at 37 °C. Supernatants were collected, peptides were further extracted twice with 5% trifluoroacetic acid in 50% acetonitrile and the supernatants were pooled. Peptide extracts were vacuum-dried, resuspended in 5 μl ddH_2O, and stored at −20 °C prior to MS analysis.

Protein identification by MALDI-TOF MS

Extracted proteins were cleaved with a proteolytic enzyme to generate peptides, then a peptide mass fingerprinting (PMF) database search following MALDI-TOF MS analysis was employed for protein identification. Briefly, 0.5 μl of the tryptic digested protein sample was first mixed with 0.5 μl of a matrix solution containing α-cyano-4-hydroxycinnamic acid at a concentration of 1 mg in 1 ml of 50% acetonitrile (v/v)/ 0.1% trifluoroacetic acid (v/v), spotted onto an anchorchip target plate (Bruker Daltonics) and dried. The peptide mass fingerprints were acquired using an Autoflex III mass spectrometer (Bruker Daltonics, Germany) in reflector mode. The algorithm used for spectrum annotation was SNAP (**S**ophisticated **N**umerical **A**nnotation **P**rocedure). This process used the following detailed metrics: peak detection algorithm: SNAP; signal to noise threshold: 25; relative intensity threshold: 0%; minimum intensity threshold: 0; maximal number of peaks: 50; quality factor threshold: 1000; SNAP average composition: averaging; baseline subtraction: median; flatness: 0.8; median level: 0.5. The spectrometer was also calibrated with a peptide calibration standard (Bruker Daltonics) and internal calibration was performed using trypsin autolysis peaks at m/z 842.51 and m/z 2211.10. Peaks in the mass range of m/z 800–3000 were used to generate a peptide mass fingerprint that was searched against the Swiss-Prot/TrEMBL database (v57.12) with 513 877 entries using Mascot software v2.2.06 (Matrix Science, London, UK). The following parameters were used for the search: *Homo sapiens*; tryptic digest with a maximum of 1 missed cleavage; carbamidomethylation of cysteine, partial protein N-terminal acetylation, partial methionine oxidation and partial modification of glutamine to pyroglutamate and a mass tolerance of 50 ppm. Identification was accepted based on significant MASCOT Mowse scores ($p < 0.05$), spectrum annotation and observed *versus* expected molecular weight and p*I* on 2-DE.

Immunoblotting

Immunoblotting was used to validate the differential abundance of mass spectrometry identified proteins. Aliquots of 20 μg of plasma proteins were diluted in Laemmli sample buffer (final concentrations: 50 mM Tris, pH 6.8, 10% (v/v)

glycerol, 2% SDS (w/v), 0.01% (w/v) bromophenol blue) and separated by 1D-SDS-PAGE following standard procedures. After electroblotting separated proteins onto 0.45 μm Immobilon P membranes (Millipore), the membranes were blocked with 5% w/v skimmed milk in TBST (50 mM Tris, pH 8.0, 150 mM NaCl and 0.1% Tween-20 (v/v)) for 1 h. Membranes were then incubated in a primary antibody solution in TBS-T containing 0.02% (w/v) sodium azide for 2 h. Membranes were washed in TBS-T (3 × 10 min) and then probed with the appropriate horseradish peroxidase-coupled secondary antibody (GE Healthcare). After further washing in TBS-T, immunoprobed proteins were visualized using an enhanced chemiluminescence method (Visual Protein Co.).

Enzyme-linked immunosorbent assay (ELISA)

ELISA was used to validate the differential abundance of mass spectrometry identified proteins. Briefly, EIA polystyrene microtitration wells were coated with 50 μg of plasma samples and incubated at 37 °C for 2 h. The plate was washed three times with phosphate buffered saline-Tween 20 (PBST) and three times with PBS. After the uncoated space was blocked with 100 μl of 5% skimmed milk in PBS at 37 °C for 2 h, the plate was washed three times with PBST. A primary antibody solution was added and incubated at 37 °C for 2 h. After washing with PBST and PBS 10 times in total, 100 μl of peroxidase-conjugated secondary antibodies in PBS was added for incubation at 37 °C for 2 h. Following 10 washings, 100 μl of 3,3′,5,5′-tetramethyl benzidine (Pierce) was added. After incubation at room temperature for 30 min, 100 μl of 1 M H_2SO_4 was added to stop the reaction followed by absorbance measurement at 450 nm using Stat Fax 2100 microtiterplate reader (Awareness Technology Inc. FL, USA).

Acknowledgements

This work was supported by grant (NSC 99-2311-B-007-002) from the National Science Council, Taiwan, NTHU Booster grant (99N2908E1) from the National Tsing Hua University and grant (VGHUST99-P5-22) from the Veteran General Hospitals University System of Taiwan. This study was also supported by the grant R99-12 from the Chiayi Christian Hospital.

References

1 L. Norgren, W. R. Hiatt, J. A. Dormandy, M. R. Nehler, K. A. Harris and F. G. Fowkes, *J. Vasc. Surg*., 2007, **45**(Suppl S.), S5–S67.
2 V. N. Varu, M. E. Hogg and M. R. Kibbe, *J. Vasc. Surg*., 2010, **51**, 230–241.
3 M. Koch, R. Trapp, W. Kulas and B. Grabensee, *Nephrol., Dial., Transplant*., 2004, **19**, 2547–2552.
4 D. P. Slovut and T. M. Sullivan, *Vascular Medicine*, 2008, **13**, 281–291.
5 A. Silvestro, N. Diehm, H. Savolainen, D. D. Do, J. Vogelea, F. Mahler, S. Zwicky and I. Baumgartner, *Vasc. Med*., 2006, **11**, 69–74.
6 K. Ono, A. Tsuchida, H. Kawai, H. Matsuo, R. Wakamatsu, A. Maezawa, S. Yano, T. Kawada and Y. Nojima, *J. Am. Soc. Nephrol*., 2003, **14**, 1591–1598.
7 A. Guerrero, R. Montes, J. Munoz-Terol, A. Gil-Peralta, J. Toro, M. Naranjo, P. Gonzalez-Perez, C. Martin-Herrera and A. Ruiz-Fernandez, *Nephrol., Dial., Transplant*., 2006, **21**, 3525–3531.
8 D. T. Ubbink, G. H. Spincemaille, R. S. Reneman and M. J. Jacobs, *J. Vasc. Surg*., 1999, **30**, 114–121.
9 J. F. Timms and R. Cramer, *Proteomics*, 2008, **8**, 4886–4897.
10 R. Westermeier and B. Scheibe, *Methods Mol. Biol*., 2008, **424**, 73–85.
11 R. Marouga, S. David and E. Hawkins, *Anal. Bioanal. Chem*., 2005, **382**, 669–678.
12 T. C. Lai, H. C. Chou, Y. W. Chen, T. R. Lee, H. T. Chan, H. H. Shen, W. T. Lee, S. T. Lin, Y. C. Lu, C. L. Wu and H. L. Chan, *J. Proteome Res*., 2010, **9**, 1302–1322.
13 H. C. Chou, Y. W. Chen, T. R. Lee, F. S. Wu, H. T. Chan, P. C. Lyu, J. F. Timms and H. L. Chan, *Free Radical Biol. Med*., 2010, **49**, 96–108.
14 H. L. Huang, H. W. Hsing, T. C. Lai, Y. W. Chen, T. R. Lee, H. T. Chan, P. C. Lyu, C. L. Wu, Y. C. Lu, S. T. Lin, C. W. Lin, C. H. Lai, H. T. Chang, H. C. Chou and H. L. Chan, *J. Biomed. Sci. (London, U. K.)*, 2010, **17**, 36.
15 J. C. de Graaff, D. T. Ubbink, D. A. Legemate, J. G. Tijssen and M. J. Jacobs, *J. Vasc. Surg*., 2003, **38**, 528–534.
16 J. Barani, J. A. Nilsson, I. Mattiasson, B. Lindblad and A. Gottsater, *J. Vasc. Surg*., 2005, **42**, 75–80.
17 L. Bertz, J. Barani, A. Gottsater, P. M. Nilsson, I. Mattiasson and B. Lindblad, *Int. Angiol*., 2006, **25**, 370–377.
18 M. Martin, A. Gottsater, P. M. Nilsson, T. E. Mollnes, B. Lindblad and A. M. Blom, *J. Vasc. Surg*., 2009, **50**, 100–106.
19 R. Marfella, C. Luongo, A. Coppola, M. Luongo, P. Capodanno, R. Ruggiero, L. Mascolo, I. Ambrosino, C. Sardu, V. Boccardi, B. Lettieri and G. Paolisso, *Atherosclerosis (Shannon, Irel.)*, 2010, **208**, 473–479.
20 N. Brechot, E. Gomez, M. Bignon, J. Khallou-Laschet, M. Dussiot, A. Cazes, C. Alanio-Brechot, M. Durand, J. Philippe, J. S. Silvestre, N. Van Rooijen, P. Corvol, A. Nicoletti, B. Chazaud and S. Germain, *PLoS One*, 2008, **3**, e3950.
21 A. Raza-Ahmad, *Biotech. Histochem*., 1994, **69**, 268–272.
22 Z. Xiaohong, C. Xiaorui, H. Jun and Q. Qisheng, *Leg. Med*., 2002, **4**, 47–51.
23 H. Balmer, F. Mahler, D. D. Do, J. Triller and I. Baumgartner, *J. Endovasc. Ther*., 2002, **9**, 403–410.
24 D. Brea, T. Sobrino, M. Blanco, M. Fraga, J. Agulla, M. Rodriguez-Yanez, R. Rodriguez-Gonzalez, d. l. O. Perez, R. Leira, J. Forteza, A. Davalos and J. Castillo, *Atherosclerosis (Shannon, Irel.)*, 2009, **205**, 561–567.
25 M. Y. Lee, S. Y. Kim, J. S. Choi, I. H. Lee, Y. S. Choi, J. Y. Jin, S. J. Park, K. W. Sung, M. H. Chun and I. S. Kim, *J. Cereb. Blood Flow Metab*., 2002, **22**, 1176–1180.
26 N. Fiotti, C. Giansante, E. Ponte, C. Delbello, S. Calabrese, T. Zacchi, A. Dobrina and G. Guarnieri, *Atherosclerosis (Shannon, Irel.)*, 1999, **145**, 51–60.
27 M. C. Cid, D. S. Grant, G. S. Hoffman, R. Auerbach, A. S. Fauci and H. K. Kleinman, *J. Clin. Invest*., 1993, **91**, 977–985.
28 H. Yin, L. Chao and J. Chao, *J. Biol. Chem*., 2005, **280**, 8022–8030.
29 J. Saez-Valero, C. Gonzalez-Garcia and V. Cena, *Mol. Brain Res*., 2003, **117**, 240–244.
30 R. A. Williams and S. E. Wilson, *Surg. Forum*, 1979, **30**, 370–372.
31 A. Bonakdarpour, S. Ming, J. L. Esterhai, P. R. Lynch, F. Reichle and H. Siplet, *J. Surg. Res*., 1976, **21**, 409–413.
32 B. L. Verges, L. Lagrost, G. Vaillant, J. M. Petit, M. Cohen, P. Gambert and J. M. Brun, *Diabetes*, 1997, **46**, 125–132.
33 L. Beinrohr, J. Dobo, P. Zavodszky and P. Gal, *Trends Mol. Med*., 2008, **14**, 511–521.
34 F. Cao, R. Hata, P. Zhu, M. Niinobe and M. Sakanaka, *Brain Res*., 2009, **1272**, 52–61.
35 G. A. Kaysen, *Blood Purif*., 2006, **24**, 51–55.
36 P. Stenvinkel, O. Heimburger and B. Lindholm, *Nephrol., Dial., Transplant*., 2004, **19**, 2181–2183.
37 P. Stenvinkel, O. Heimburger, F. Paultre, U. Diczfalusy, T. Wang, L. Berglund and T. Jogestrand, *Kidney Int*., 1999, **55**, 1899–1911.
38 W. F. Owen and E. G. Lowrie, *Kidney Int*., 1998, **54**, 627–636.
39 P. Stenvinkel, O. Heimburger, B. Lindholm, G. A. Kaysen and J. Bergstrom, *Nephrol., Dial., Transplant*., 2000, **15**, 953–960.
40 H. L. Chan, S. Gharbi, P. R. Gaffney, R. Cramer, M. D. Waterfield and J. F. Timms, *Proteomics*, 2005, **5**, 2908–2926.
41 S. Gharbi, P. Gaffney, A. Yang, M. J. Zvelebil, R. Cramer, M. D. Waterfield and J. F. Timms, *Mol. Cell. Proteomics*, 2002, **1**, 91–98.

